Modeling of the loading path dependent magnetomechanical behavior of Galfenol alloy*

Hui Jiang(江慧) and Jie Zhu(朱洁)†

State Key Laboratory of Advanced Metals and Materials, University of Science and Technology Beijing, Beijing 100083, *China*

(Received 11 October 2016; revised manuscript received 26 December 2016; published online 13 February 2017)

The magnetomechanical behavior of single-crystal Galfenol alloy was found to be strongly dependent on the loading paths. An energy-based anisotropic domain rotation model, assuming that the interaction between domains can be ignored and the probability of the magnetic moment pointing along a particular direction is related to the free energy along this direction, is used to simulate the magnetostriction versus magnetic field and stress curve and to track the magnetic domain motion trail. The main reason for loading path dependent effect is the rotation/flipping of the magnetic domains under different loading paths. The effect of loading and unloading paths on 90° magnetic domain motion was studied by choosing different loading and unloading state and paths. The results show that prior loading magnetic field can make the 90° magnetic domains flip to the directions of 45° domains because the magnetic field is the driving force to make the domains rotate, and the final loading state and the loading path both have great influence on the motion of 90° magnetic domains.

Keywords: magnetomechanical behavior, loading path dependent, 90° magnetic domain flipping

PACS: 75.80.+q **DOI:** 10.1088/1674-1056/26/3/037503

1. Introduction

Fe–Ga alloys are considered as promising materials which can be widely used in actuators and sensors due to their large saturated magnetostriction in low applied magnetic field and good mechanical property. In previous study, most experiments carried out to study the magnetomechanical behavior of Galfenol were about measuring either magnetostriction under constant pre-compressive stress or stress–strain behavior under constant magnetic field.[1–3] However, when used as actuators and sensors, the Fe–Ga alloys always work under complicated magnetic and stress loading condition, which is different from the experimental loading condition in laboratory. So the study of magnetomechanical behavior of Galfenol alloy under complex loading condition is necessary and meaningful.

A phenomenological magnetomechanical hysteresis model which considered the influence of past loading history by using some path-dependent differentials has been developed by Bergqvist. The calculation results were compared with the experimental observation, including the strain and magnetization curves at constant magnetic field or constant stress.[4] Pei has studied the path-dependent deformation behaviors of Terfenol-D under two types of magnetomechanical loadings and found that the stress and the magnetic field have different influence on the domain distribution. He used the domain switch process to explain this phenomenon, which is a phenomenological analysis.[5] In order to study the Galfenol mechanical–magnetic coupling coefficients, Yoo conducted two types of closed-loop cyclic loading on Galfenol samples and measured the magnetostriction and magnetization as a function of magnetic field and compressive stress. He established an experimental procedure to exam magnetomechanical cycles and evaluated the energy balances.[6]

In this paper, Jiles–Thoekle model[7] was used to simulate the magnetomechanical behaviors of single crystalline Galfenol under different loading paths. In order to explore the reason of magnetomechanical behavior subject to loading path, a series of loading paths were designed to calculate the magnetostriction, the domain switch process, and the energy distribution. This work is beneficial to deeply understand the effect of magnetic field and compressive stress on domain switch process and to model the magnetomechanical behavior under complicated magnetomechanical loading condition.

2. Model

Based on the Stoner–Wohlfarth assumption that the interaction between domains can be neglected,[8] Jiles and Thoekle[7] proposed a model that gave the free energy of a material and tracked the location of local energy minima in the orientation of magnetic domains under the action of changing magnetic field and applied stress. But the magnetostriction versus magnetic field and stress curves simulated by this model are broken lines. Armstrong[9] extended Jiles–Thoekle model by assuming that the distribution of the magnetization moment depends on the free energy, which can help get a smooth and qualitatively accurate magnetostriction curves.

For a material with cubic structure under applied magnetic field and stress, the total magnetic free energy of a unit volume of magnetization within a single crystal consists of

*Project supported by the General Program of National Natural Science Foundation of China (Grant No. 51371028).

†Corresponding author. E-mail: jiezhu@ustb.edu.cn

© 2017 Chinese Physical Society and IOP Publishing Ltd

magnetocrystalline anisotropy energy, static magnetic energy, and magnetoelastic energy, reading

$$E_t = E_K + E_H + E_\sigma, \tag{1}$$

$$E_K = K_1\left(\alpha_x^2\alpha_y^2 + \alpha_x^2\alpha_z^2 + \alpha_y^2\alpha_z^2\right), \tag{2}$$

$$E_H = -\mu_0 M_s H\left(\alpha_x\beta_x + \alpha_y\beta_y + \alpha_z\beta_z\right), \tag{3}$$

$$E_\sigma = -\tfrac{3}{2}\lambda_{100}\sigma\left(\alpha_x^2\gamma_x^2 + \alpha_y^2\gamma_y^2 + \alpha_z^2\gamma_z^2\right) - 3\lambda_{111}\sigma\left(\alpha_x\alpha_y\gamma_x\gamma_y + \alpha_y\alpha_z\gamma_y\gamma_z + \alpha_x\alpha_z\gamma_x\gamma_z\right), \tag{4}$$

where α_i, β_i, and γ_i $(i = x, y, z)$ are the direction cosine of the magnetization, applied magnetic field, and applied stress, respectively. In this calculation, the directions of the applied magnetic field and stress are identical, both along [110] direction, so $\beta_i = \gamma_i$. K_1 is the magnetocrystalline anisotropy coefficient which is an intrinsic parameter relating to the material composition and processing method.[3,10] H is the magnetic field strength and σ is the applied stress. λ_{100} and λ_{111} are magnetostriction resulting from the rotation of a fully random magnetization state into a fully oriented [100] or [111] direction, respectively.

Magnetocrystalline anisotropy energy E_k is a resistance of domain rotation, preventing domains switching away from the original easy axis direction. The static magnetic energy E_H is a driving force to make the magnetization moment rotate away from the original direction to the direction of magnetic field. The magnetoelastic energy E_σ comes from the interaction of applied stress and the stress resulting from magnetic moments rotation. Both the magnetic field and applied stress can greatly change the spatial distribution of free energy, affecting the location of energy minima.

We assume that the FeGa single crystal is composed of a large number of equivalent magnetization units, each of which has a particular orientation of magnetization with a particular probability. According to the Armstrong assumption,[9] for any direction, the probability of the magnetization depends on the total free energy corresponding to that direction, that is,

$$P_i = \frac{\mathrm{e}^{-E_{t,i}/\omega}}{\sum_i \mathrm{e}^{-E_{t,i}/\omega}}, \tag{5}$$

where $E_{t,i}$ is the total free energy in ith direction and ω is the energy distribution parameter which signifies the extent of imperfections in the crystal.[3] From Eq. (5), it can be seen that the value of ω has great influence on the change of fractions of each domains.

The total magnetostriction in any crystallographic direction can be calculated by summing up the contribution of all domains in each direction,

$$\lambda = \sum_i P_i\left[\frac{3}{2}\lambda_{100}\left(\alpha_{i,x}^2\beta_{\mathrm{m},x}^2 + \alpha_{i,y}^2\beta_{\mathrm{m},y}^2 + \alpha_{i,z}^2\beta_{\mathrm{m},z}^2 - \frac{1}{3}\right) + 3\lambda_{111}\left(\alpha_{i,x}\alpha_{i,y}\beta_{\mathrm{m},x}\beta_{\mathrm{m},y} + \alpha_{i,x}\alpha_{i,z}\beta_{\mathrm{m},x}\beta_{\mathrm{m},z} + \alpha_{i,y}\alpha_{i,z}\beta_{\mathrm{m},y}\beta_{\mathrm{m},z}\right)\right], \tag{6}$$

where $\alpha_{i,j}$ $(j = x, y, z)$ are the direction cosines of the magnetization along the ith direction and the $\beta_{\mathrm{m},j}$ $(j = x, \mathrm{y}, \mathrm{z})$ are the direction cosines of the measuring direction.

In this model, it is proposed that the sample used to calculate is a single crystal of $Fe_{82}Ga_{18}$ alloy in rod shape, and the directions of magnetic field, compressive stress, and measurement are all along the [110] direction. In the calculation, the parameters used in the model[3,11–13] are listed in Table 1.

Table 1. The parameters used in the model.

K_1	K_2	$\mu_0 M_s$	λ_{100}	λ_{111}	ω
3.6×10^4 J·m^{-3}	0 J·m^{-3}	1.5 T	267×10^{-6}	5×10^{-6}	920 m^{-3}

3. Results and discussion

3.1. Loading process

For each loading state, two different loading sequences of stress and magnetic field are employed, as shown in Fig. 1: one is magnetic-and-stress sequence (O–A–B) and the other is stress-and-magnetic field sequence (O–A′–B).

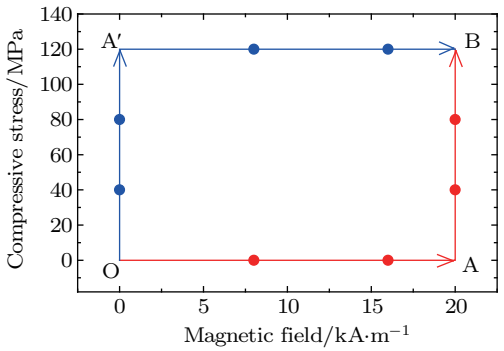


Fig. 1. Two stress–magnetic field loading paths.

Setting up a series of final loading states, the magnetomechanical behavior under various compressive stress and magnetic field with two types of loading sequences is simulated. Figures 2(a) and 2(b) are the results of loading sequences O–A–B and O–A′–B, respectively. The results of Figs. 2(a) and 2(b) are put together to compare the difference as given in Fig. 2(c). It can be clearly seen that the magnetostriction results under two loading sequences are not totally identical with great distinct difference in a certain region of loading states, which means that the magnetostriction is path dependent. By comparing the difference in Fig. 2(c), the stress and magnetic field can be divided into three regions, as shown in Fig. 2(d). In regions 1 and 2, for both loading sequences their magnetostrictions have the same value, while in loading region 3 the magnetostrictions have distinct difference.

From Fig. 2(a), it can be seen that after applying magnetic field the material has magnetostrictive elongation. With the increase of magnetic field, the magnetostriction enlarges until it

reaches to a saturated value. Then the deformation changes when compressive stress is loaded. As Fig. 2(b) shows, when the compressive stress is applied, the alloy has magnetostrictive shortening due to the domain motion to the directions perpendicular to the stress. As the stress increases, the shortening amount changes until the domain motion reaches the saturated state, which is consistent with the previous study. Under the larger pre-stress, the greater magnetic field is needed to make the alloy magnetostrictive elongation and reach magnetostrictive saturation.

When both the magnetic field and stress are small, as the right part of region 1 in Fig. 2(d) shows, the free energy surface distortion caused by them is not too serious and the domain motion trail is mainly affected by the magnetocrystalline anisotropy energy,[14] so both loading sequences can get the same results with gradual reversible rotation of magnetic domain. When the compressive stress is large but the magnetic field is small, as the left part of region 1 in Fig. 2(d) shows, the modeled results under both loading paths also are identical because of the dominant effect of stress.[14] When the magnetic field is large enough as region 2 in Fig. 2(d), to make all the magnetic domains rotate to the magnetic field direction, both the two loading sequences can get the same result.

However, when both the magnetic field and compressive stress are large in region 3 of Fig. 2(d), the two loading sequences have different magnetostriction results. If the magnetic field is loaded firstly, when the magnetic field is larger than 16 kA/m, the magnetostriction of Galfenol at every stress is nearly saturated even after loading big compressive stress as shown in Fig. 2(a). But if the compressive stress is loaded prior to magnetic field, the magnetostriction behavior has some distinct difference. This is resulting from the competition of the magnetocrystalline anisotropy energy and magnetoelastic energy. For the loading sequence O–A–B, the firstly loading of magnetic field can make all the domains rotate to saturated state and keep in this state even after loading compressive stress. But for O–A′–B, after loading large compressive stress, almost all domains rotate to the directions perpendicular to the stress direction, and the domains are hard to rotate to magnetic field direction in the following magnetic field loading.

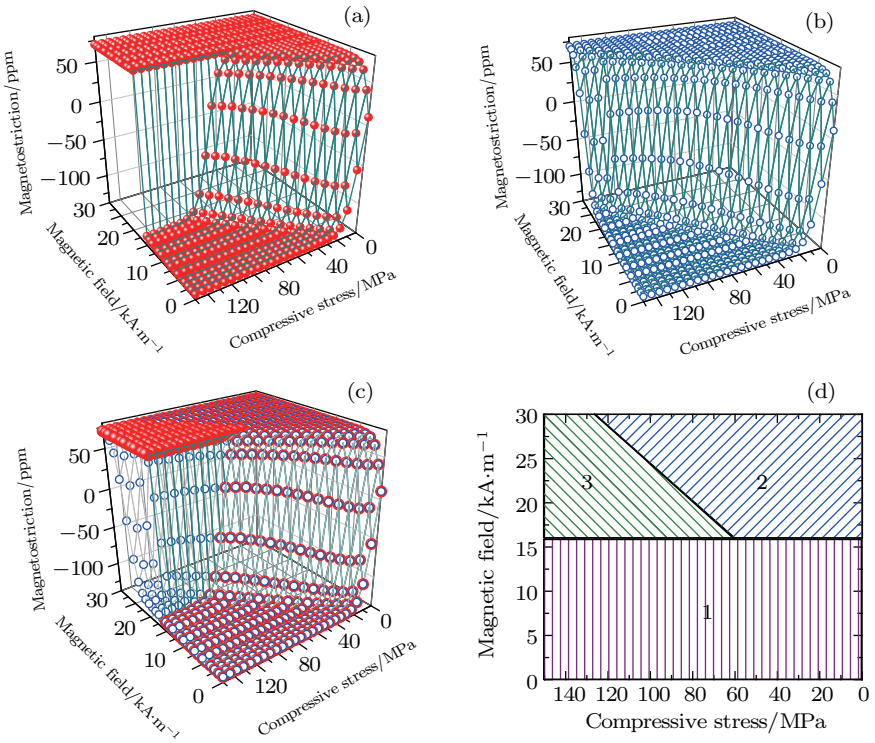


Fig. 2. The magnetostriction at different stress and magnetic fields under the two types of loading paths: (a) O–A–B and (b) O–A′–B. (c) Comparison of the two cases of panels (a) and (b). (d) The loading area division according to panel (c).

In order to compare the influence of loading path on the magnetomechanical behavior and find the reason for this path-dependent effect, a final loading state ($H = 20$ kA/m, $\sigma = 120$ MPa) was chosen, which is in the region 3 of Fig. 2(d) having obviously different magnetostrictive behavior. From Fig. 2, it can be seen that at this final loading state, the magnetostriction of loading sequence O–A–B is about 70 ppm, while the other loading path O–A′–B is 7 ppm.

At the same time, the domain motion trails were tracked under the loading process, and the modeled domain motion trails in the six directions are given in Fig. 3. For the loading sequence O–A–B, with the loading direction of [110], when

the magnetic was given and increased, the magnetic domains gradually rotated away from their original axes. When the magnetic increased to a certain value, the 90° domains along [001] and [00-1] directions and the two 45° domains nearly [0-10] and [-100] directions jumped/flipped to the [100] and [010] directions respectively, which directions are close to the loading direction [110]. These domain flippings correspond to different magnetic field thresholds. Even after loading the compressive stress, all these magnetic domains were still along these two directions [100] and [010]. Compared with the domain rotation paths of O–A–B, the most obvious difference case in loading path O–A′–B is that during the whole loading process, no 90° domain was found jumping to the direction of 45° domains. It can be concluded that the path dependent effect is caused by the rotation/flipping of 90° domains.

The three-dimensional free energy surface change process of the two loading paths is shown in Fig. 4, which presents the anisotropy of free energy under each loading state. The energy is proportional to the radius at each direction. The crystallographic directions are represented on the diagrams for reference. The loading states are selected from the two loading sequence as the round spots of Fig. 1 show. Obviously, the distortion of the free energy surface caused by the applied stress and magnetic field are different. It can be seen that the evolution of energy minima highly depends on the loading sequences, which means that the loading sequence can affect the domain motion trail.

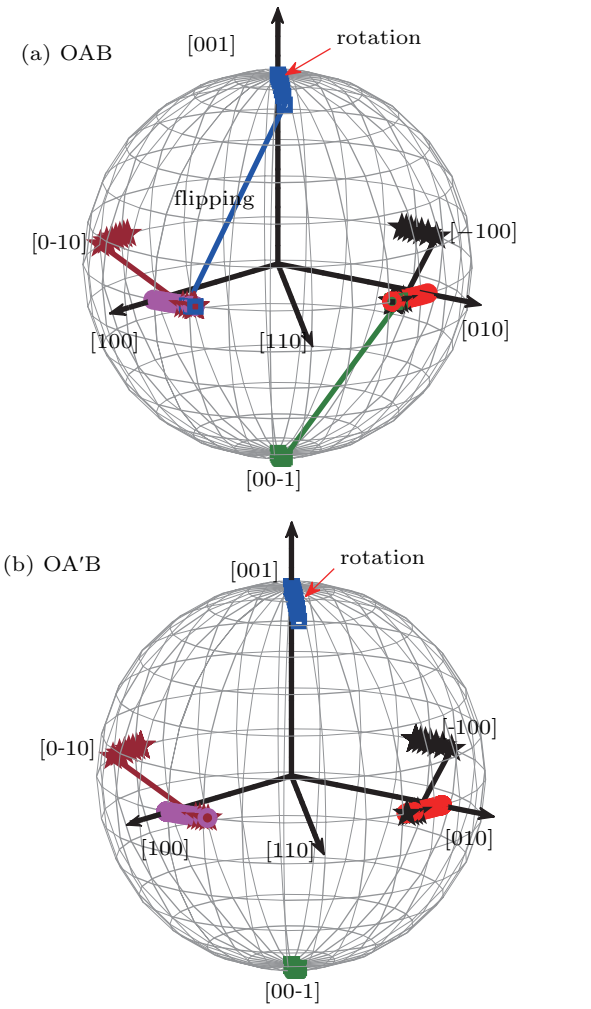


Fig. 3. The domain rotation paths in response to the two loading paths (a) O–A–B and (b) O–A′–B.

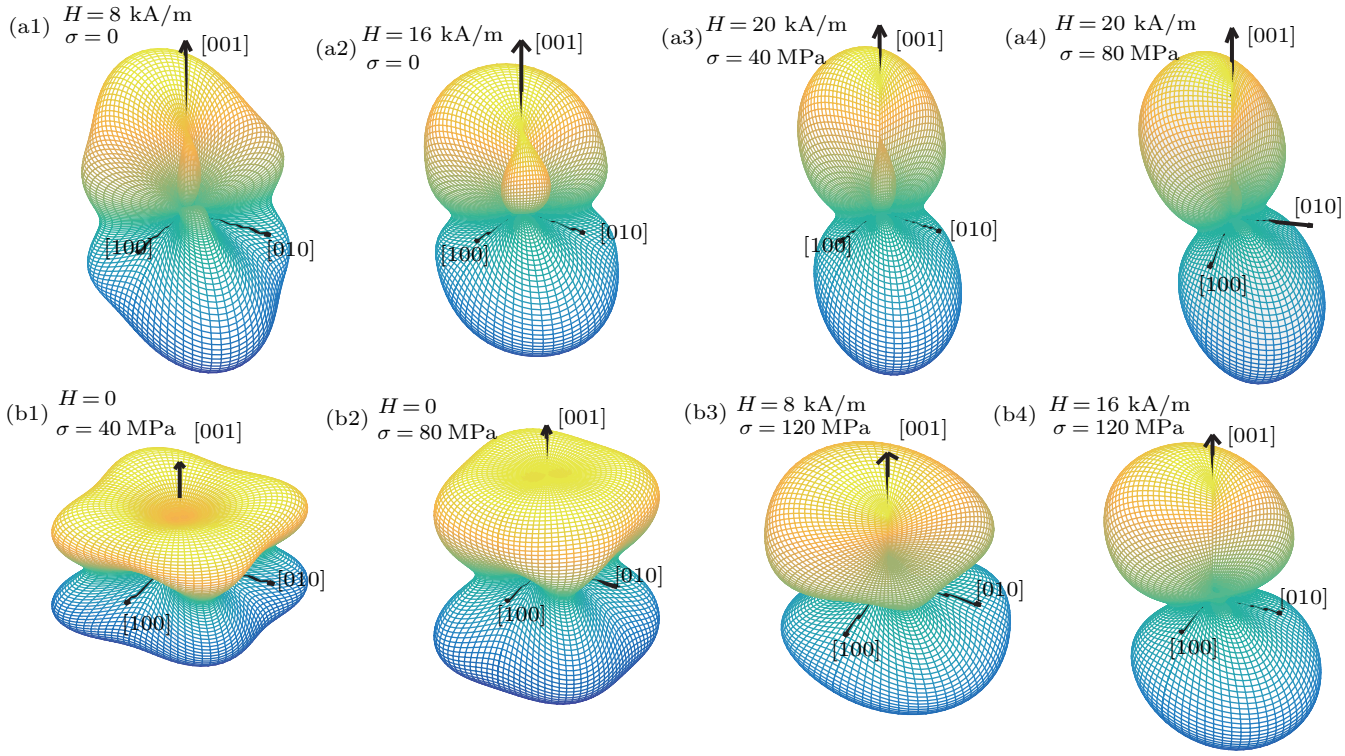


Fig. 4. The energy surface change at different magnetic field and stress under the two loading paths sequentially.

In order to study the factors affecting path dependent effect, three more different final loading states were selected, which were A ($H = 21$ kA/m, $\sigma = 60$ MPa), B ($H = 25$ kA/m, $\sigma = 60$ MPa), and C ($H = 25$ kA/m, $\sigma = 73$ MPa). It was assumed that the loading paths before $H = 20$ kA/m, $\sigma = 50$ MPa were the same, and then there are three paths selected toward to each final loading state. The three loading conditions with three different paths are illustrated in Fig. 5, respectively.

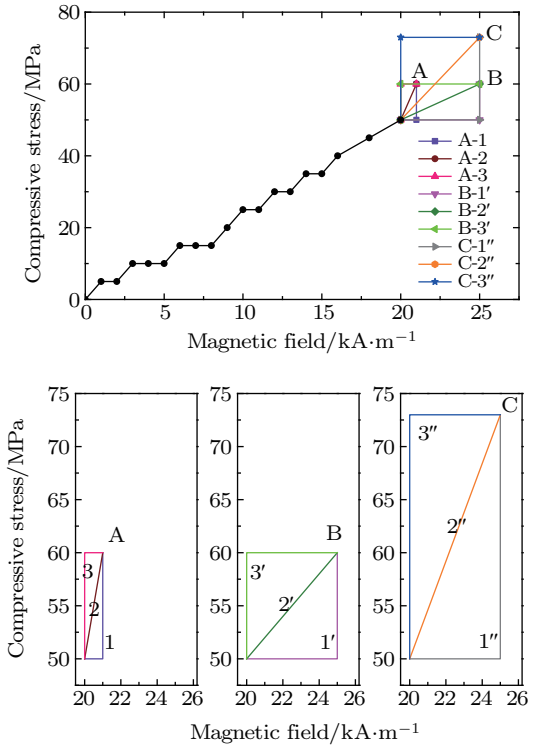


Fig. 5. Three loading paths towards to three different loading states.

At the loading state $H = 20$ kA/m, $\sigma = 50$ MPa, all paths have the same magnetic domain configuration. But after this loading state, the magnetic domain configuration strongly depends on each loading path. Simulating the domain distribution under the loading magnetic fields and stresses, the 90° domain rotation/jump trail in these nine paths can be modeled. Table 2 shows the cases of whether the 90° magnetic domain flipped during each loading path. Compared the calculated results of the nine paths in Table 2, it can be found that the loading path and the value of magnetic field and stress have great influence on the motion of 90° domains. Before the magnetic field and stress increased to 20 kA/m and 50 MPa respectively, the 90° domains rotated gradually. During the three paths (1, 2, 3) to A loading state, no 90° domain flipping happens. But if the loading state is B, for the three loading paths (1′, 2′, 3′), the 90° magnetic domains can flip to the directions of 45° domains. When it is C loading state, only the loading path 1″ made the 90° magnetic domains flipping, which is because as the compressive stress increased the domain flipping resistance resulting from magnetoelastic energy increased. While for the other loading paths 2″ and 3″, the increased stress are too big to make the 90° domains flip. From the analysis above, it can be concluded that the loading paths, include loading sequence and magnitude of loading, have great effect on the domain motion trail.

Table 2. The results of 90° domain flipping along three types of loading sequences.

Loading states	Flipping of 90° domain
A (21 kA/m, 60 MPa)	1, 2, 3 NO
B (25 kA/m, 60 MPa)	1′, 2′, 3′ YES
C (25 kA/m, 73 MPa)	1″ YES, 2″, 3″ NO

The sensing and actuating behaviors of the FeGa alloy corresponding to the two loading sequences in Fig. 1 are also considered. For single crystal FeGa sample with 18 at.% Ga, its Young's module in the [110] direction is expected to be 150 GPa.[15] Considering the elastic deformation of Fig. 2(a), the stress–strain deformation curves under different magnetic field can be simulated, as shown in Fig. 6(a). When the magnetic field is zero, during the first period of loading, the stress–strain curves is not linear because of the contribution of magnetostriction caused by stress. After all the domain rotation caused by stress reaches to saturated state, the strain deformation is only elastic deformation which is linear. In the case of applying a magnetic field, at the beginning of loading compressive stress, the deformation presents linear curves until the stress increases to threshold value, marked by in Fig. 6. The magnetoelastic energy can overcome the resistance of static energy to make the domain rotate, and the deformation is composed of magnetostriction and elastic deformation. As the magnetic field increases, the larger compressive stress is needed to make the domain rotate. When the domain rotation caused by stress is saturated, the strain deformation is elastic deformation. The bigger magnetic field applied is, the greater the compressive stress value (marked by □ in Fig. 6) is needed to make deformation back to linear. This simulation agrees well with the results of the sensing characteristics of 18.4 at.% Ga at different bias magnetic fields,[11] which means that our simulation model and results are reliable.

Figure 6(b) is the simulated magnetostriction–magnetic field curves under different pre-stresses chose from the results of Fig. 2(b). It can be seen that if preloading was 12 MPa, which was not enough to make all the magnetic domain turn to 90° domain, later added magnetic field cannot gain largest saturation magnetostriction value. When the preloading stress was large enough, such as 30 MPa or bigger, the saturated magnetostriction can reach up to the maximum value. It is worth noting that as the pre-stress increases, both the critical magnetic fields for magnetostrictive elongation and mag-

netostrictive saturation increase. The overall trend and characteristic of Fig. 6(b) are in accordance with the experimental results of Fe–Ga in Refs. [16] and [17]. Our calculation results are partly consistent with the experimental results of single-crystal $Fe_{82}Ga_{18}$ in Ref. [17] which gives the λ–H curves at 0, 30, 60, and 80 MPa compressive stresses. Compared with the strain under zero stress, the saturated magnetostrictions under the other three stresses increase by about 130 ppm and the saturated magnetic field increased to 6.4 kA/m, 13 kA/m, and 16 kA/m, respectively, which agree well with our simulated result. It should be noted that because the parameters chosen in our calculation may not be very suitable for the material used in literature, the saturation magnetostriction we get does not fit the experiments well. As Yan mentioned,[18] some parameters used in calculation should be got from actual material to get more accurate simulation result because of the properties inconsistency of magnetostictive material. This let us know that in the future simulation we should choose more suitable parameters based on actual material.

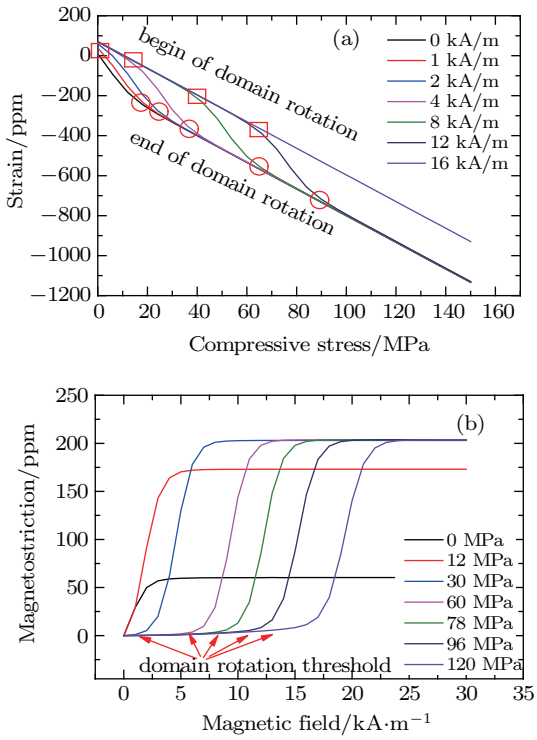


Fig. 6. (a) The simulated stress–strain curves at different pre-magnetic field and (b) the magnetic field–magnetostriction curves at different pre-stresses.

3.2. Unloading process

In a real application, the unloading process is inevitable and must be considered. The effect of unloading path on magnetic domain motion has been studied by adding different unloading paths after loading to form a cycle loading loop, as shown in Fig. 7. Four loading sequences have been considered, which are O–A–B–A′–O, O–A′–B–A–O, O–A–B–A–O, and O–A′–B–A′–O.

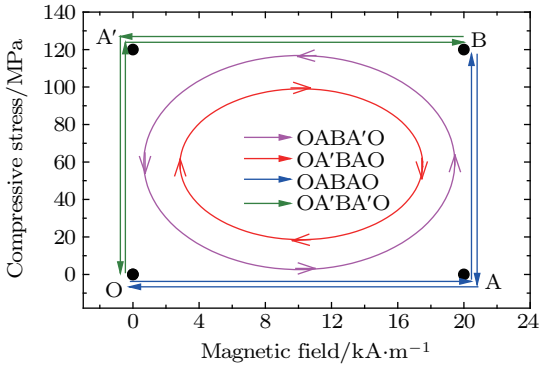


Fig. 7. Four loading and unloading sequences.

The final loading state B is chosen as $H = 20$ kA/m and $\sigma = 120$ MPa, then unloading to zero along the four sequences in Fig. 7. Tracking down the magnetic domain motion trails during unloading process, the results are illustrated in Fig. 8. For the loops O–A–B–A′–O and O–A–B–A–O which have the same loading sequence O–A–B, during the loading process the two 45° magnetic domains along [-100] and [0-10] directions and the 90° magnetic domains flip to the other two 45° magnetic domains directions as shown in Fig. 3(a). But in the unloading processes B–A′–O and B–A–O, all these domains gradually rotate to the [100] and [010] directions with no magnetic domains flipping. Although the two loading paths have different unloading sequences, they have similar domain motion trails. It can be inferred that the flipping of 90° magnetic domains is irreversible because they cannot flip back to be 90° domains again along the two unloading paths.

For the other two loops O–A′–B–A–O and O–A′–B–A′–O having the same loading sequence O–A′–B, only the two 45° magnetic domains along [-100] and [0-10] directions flip to other two 45° domains directions with gradual rotation of 90° domains during the loading process O–A′–B as illustrated in Fig. 3(b). But in the following unloading sequences B–A–O and B–A′–O, these two unloading sequences show different domain motion trails. For O–A′–B–A–O, during the unloading process, the two 90° domains can flip to the 45° magnetic domains directions, while for O–A′–B–A′–O the 90° domains just gradually rotate back along their motion trails of loading process. It is worth noting that three sequences of the four, O–A–B–A′–O, O–A–B–A–O, and O–A′–B–A–O, have the same domain configuration when the stress and magnetic field were removed at last, and that for the four loading loops their domain distributions after unloading are different from their original domain distributions before loading. The domain motion trails of the four sequences in Fig. 8 indicate that the loading history and the unloading sequence have great effect on the domain motion. During the piezomagnetic and magnetoelastic processes, the motion of magnetic domains has hysteresis and transition effects (i.e., domain flipping mentioned in this paper), and the hysteresis effect of magnetization is always

induced by the irreversible transitions of domain motion[19] which involves the energy loss. In this simulation, it is found that the motion of magnetic domains being reversible or irreversible is dependent on the loading and unloading sequence, which means that the hysteresis behavior is related to the loading method.

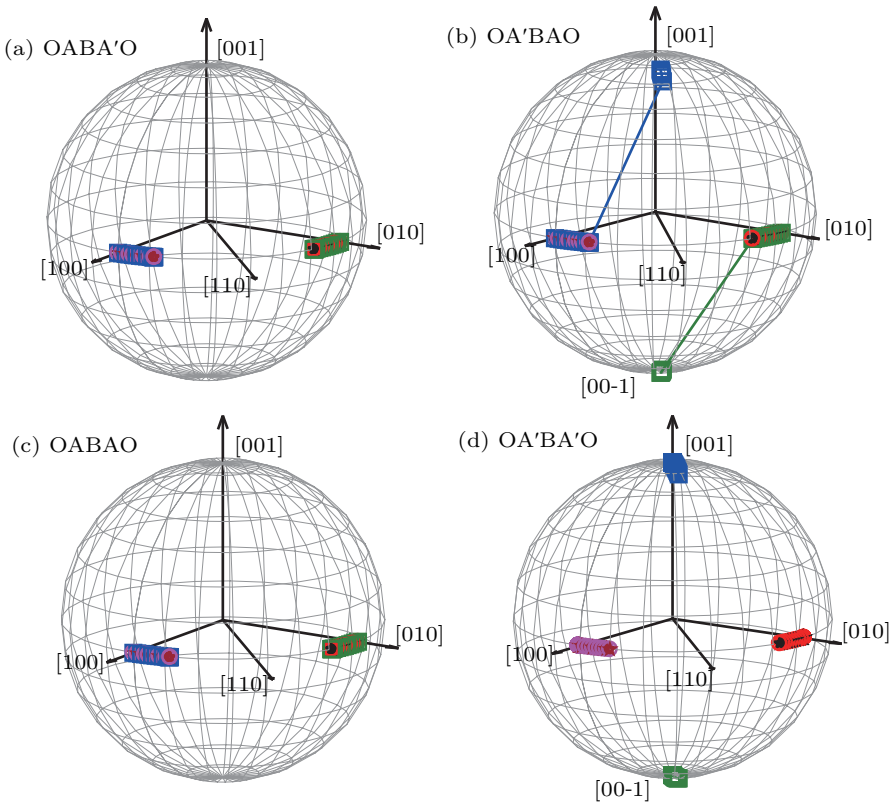


Fig. 8. The domain rotation paths under the four unloading sequences.

There are more unloading paths based on the loading process in Fig. 9 designed to study the effect of unloading paths on domains motion. Figure 9 shows the eight unloading paths with different magnetic field and stress offloading from two final loading states. From the previous calculation, it has been known that at the final loading point A (20 kA/m, 50 MPa) the directions of 90° magnetic domains are still close to their original directions with no flipping, while at the point of B (25 kA/m, 60 MPa) the 90° magnetic domains have flipped to the 45° domain directions. All the eight unloading paths are simulated to get their magnetic domains distribution, which are shown in Table 4. Compared the results of the four unloading paths after loading state A (20 kA/m, 50 MPa), it can been seen that along the two unloading paths 1 and 2, 90° domains flipping can happen, while for the other two unloading paths all the domains only can rotate gradually, which means that the unloading paths have great influence on the domains movement. For the loading state of B (25 kA/m, 60 MPa) at which the 90° domains have flipped to the directions of 45° domains, the 90° magnetic domains cannot flip along all the four unloading paths. What is more, many more unloading magnetic field and stress groups have been modeled for this loading state, but they all do not have 90° magnetic domains flipping. That is to say, for the loading point B (25 kA/m, 60 MPa), there will be no 90° magnetic domains flipping to happen no matter what the unloading magnetic field and stress are.

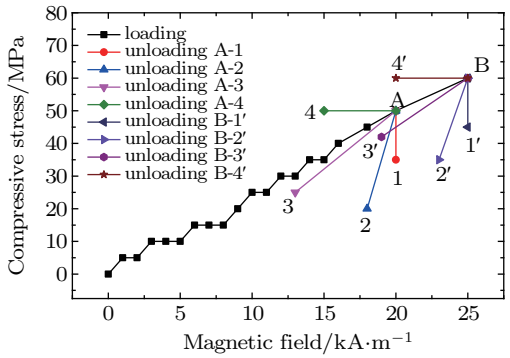


Fig. 9. Unloading paths from two points.

Table 3. The results of domain movement after unloading with different magnetic fields and stresses.

Final loading state	Unloading path	Domain movement
A (20 kA/m, 50 MPa)	1 and 2	have 90° magnetic domains flipping
	3 and 4	have no magnetic domains flipping
B (25 kA/m, 60 MPa)	all	have no magnetic domains flipping

4. Conclusion

The magnetostrictive behavior of Galfenol is loading path dependent. It has been found that in certain loading state, different loading paths have the same magnetostrictive behavior, while in some loading state they lead to distinct different behavior.

The energy surface change process and the domain motion trail both illustrate the reason of path dependent effect. It is found that the path-dependent effect results from the competitive effect of magnetoelastic energy and static magnetic energy on domain motion.

The motion patterns (rotation/flipping) of 90° magnetic domain are different along different loading path, leading to different domain configurations at the same final applied field. The domain distribution, loading path, and unloading path all have great effect on the domain motion, especially on the flipping of 90 ° magnetic domains.

An extended model based on Jiles–Thoekle model and Armstrong assumption is used to simulate the stress–strain curves and magnetostriction curves under two extreme loading sequences, and the simulation results agree well with the experimental observations in literatures. However, the realistic loading conditions are much more complex. This model may then be used as a tool to predict the magnetostrictive behavior under realistic loading condition.

References

[1] Zhao X, Mellors N and Lord D G 2007 *J. Appl. Phys.* **101** 09C513
[2] Clark A E, Yoo J H, Cullen J R, Wun-Fogle M, Petculescu G and Flatau A 2009 *J. Appl. Phys.* **105** 07A913
[3] Atulasimha J, Flatau A and Cullen J R 2008 *Smart Mater. Struct.* **17** 025027
[4] Bergqvist A and Engdahl G 1994 *J. Appl. Phys.* **75** 5496
[5] Pei Y M and Fang D N 2008 *Mater. Lett.* **62** 1313
[6] Yoo J H, Pelligrini G, Datta S and Flatau A 2011 *Smart Mater. Struct.* **20** 075008
[7] Jiles D C and Thoekle J B 1994 *J. Magn. Magn. Mater.* **134** 143
[8] Stoner E C and Wohlfarth E P 1948 *Philos. Trans. R. Soc. London, Ser. A* **240** 599
[9] Armstrong W D 1997 *J. Appl. Phys.* **81** 2321
[10] Restorff J B, Wun-Fogle M, Clark A E and Hathaway K B 2006 *IEEE Trans. Magn.* **42** 3087
[11] Atulasimha J, Flatau A B and Summers E 2007 *Smart Mater. Struct.* **16** 1265
[12] Clark A E, Hathaway K B, Wun-Fogle M, Restorff L B, Lograsso T A, Keppens V M, Petculescu G and Taylor R A 2003 *J. Appl. Phys.* **93** 8621
[13] Kellogg R A, Flatau A B, Clark A E, Wun-Fogle M and Lograsso T A 2002 *J. Appl. Phys.* **91** 7821
[14] Liu J H, Wang Z H, Jiang C B and Xu H B 2010 *J. Appl. Phys.* **108** 033913
[15] Kellogg R A 2003 *Development and Modeling of Iron-Gallium Alloys* (Ph. D. Dissertation) (Ames: Iowa State University)
[16] Wun-Fogle M, Restorff J B and Clark A E 2006 *J. Intell. Mater. Syst. Struct.* **17** 117
[17] Atulasimha J, Akharas G and Flatau A B 2008 *J. Appl. Phys.* **103** 07B336
[18] Yan B P, Zhang C M, Li L Y, Tang Z F, Lü F Z and Yang K J 2015 *Acta Phys. Sin.* **64** 027501 (in Chinese)
[19] Yan B P, Zhang C M, Li L Y, Lü F Z and Deng S 2016 *Acta Phys. Sin.* **65** 067501 (in Chinese)